Science Letters:

New solutions of shear waves in piezoelectric cubic crystals

ZAKHARENKO A.A.

(*International Institute of Zakharenko Waves, Krasnoyarsk-37, 17701, Krasnoyarsk 660037, Russia*)

E-mail: aazaaz@inbox.ru

Abstract: Acoustic wave propagation in piezoelectric crystals of classes $\overline{4}3m$ and 23 is studied. The crystals Tl_3VS_4 and Tl_3TaSe_4 $(\overline{4}3m)$ of the Chalcogenide family and the crystal $Bi_{12}TiO_{20}$ (23) possess strong piezoelectric effect. Because the surface Bleustein-Gulyaev waves cannot exist in piezoelectric cubic crystals, it was concluded that new solutions for shear-horizontal surface acoustic waves (SH-SAWs) are found in the monocrystals using different electrical boundary conditions such as electrically "short" and "open" free-surfaces for the unique [101] direction of wave propagation. For the crystal Tl_3TaSe_4 with coefficient of electromechanical coupling (CEMC) $K_e^2 = e^2/(C \times g) \sim 1/3$, the phase velocity V_{ph} for the new SH-SAWs can be calculated with the following formula: $V_{ph} = (V_a + V_t)/2$, where V_t is the speed of bulk SH-wave, $V_t = V_{t4}(1 + K_e^2)^{1/2}$, $V_a = a_K V_{t4}$, $a_K = 2[K_e(1 + K_e^2)^{1/2} - K_e^2]^{1/2}$, and $V_{t4} = (C_{44}/\rho)^{1/2}$. It was found that the CEMC K^2 evaluation for Tl_3TaSe_4 gave the value of $K^2 = 2(V_f - V_m)/V_f \sim 0.047$ (~4.7%), where $V_f \sim 848$ m/s and $V_m \sim 828$ m/s are the new-SAW velocities for the free and metallized surfaces, respectively. This high value of $K^2(Tl_3TaSe_4)$ is significantly greater than $K^2(Tl_3VS_4) \sim 3\%$ and about five times that of $K^2(Bi_{12}TiO_{20})$. PACS: 51.40.+p, 62.65.+k, 68.35.Gy, 68.35.Iv, 68.60.Bs, 74.25.Ld.

INTRODUCTION

The shear-horizontal surface acoustic waves (SH-SAWs) were theoretically distinguished from the bulk SH-waves by Bleustein (1968) and Gulyaev (1969) simultaneously at the end of the 1960s. The surface Bleustein-Gulyaev (BG) waves (Bleustein 1968; Gulyaev, 1969), possessing a hybridization between the mechanical displacement U_2 and the electric potential $\varphi = U_4$, can propagate on some surface cuts of the transversely-isotropic crystals of the hexagonal and tetragonal classes when propagation directions are perpendicular to an odd-order symmetry axis. It was recently noted by Gulyaev and Hickernell (2005) that SH-SAWs cannot exist in piezoelectric cubic crystals. Kessenikh and Shuvalov (1982) also discusses that SH-SAWs on electrically open or shorted surfaces of piezoelectric crystals of symmetry classes 622 and 422 cannot exist if the propagation direction is perpendicular to six- or four-fold axis.

However, when the transversely-isotropic symmetry decreases from 622 to 6 or from 422 to 4 classes, the surface BG-waves can be found. In addition, Maerfeld and Tournois (1971) discovered new possibilities for shear-horizontal waves propagating along the interface between two opposite-polarized similar piezoelectric materials as well as between two dissimilar ones. It is noted that both the surface BG-wave and interfacial electroacoustic Maerfeld-Tournois (MT) wave may be caused by interfacial crack propagation between two dissimilar piezoelectric crystals. Note that the interfacial MT-waves, like the surface BG-waves, can exist in transversely-isotropic piezoelectrics.

This paper is aimed to report theoretical study of surface SH-waves in piezoelectric cubic crystals with the strong piezoelectric effect. The Chalcogenide family (Tl_3VS_4 and Tl_3TaSe_4) (Henaff *et al.*, 1982) are soft crystals belonging to the cubic class $\overline{4}3m$ and possessing both zero temperature coefficients and

strong piezoelectric coupling. In spite of their very large potential interest, especially for moderate frequency and large bandwidth, such ternary thallium Chalcogenides are not commercially available—probably due to their mechanical softness and fabrication difficulties. In contrast to the Chalcogenides, the piezoelectric ceramics of the point group symmetry 23 [$Bi_{12}SiO_{20}$ and $Bi_{12}GeO_{20}$ (Kamenov *et al.*, 2000; Zakharenko, 2005), and $Bi_{12}TiO_{20}$ (Kamenov *et al.*, 2000)] can be used in piezoelectronics.

THEORY

Fig.1 introduces a rectangular coordinate system (x_1, x_2, x_3), with the x_1Ox_3 sagittal plane being perpendicular to the lowest odd-order symmetry axis of a piezoelectric cubic crystal with the x_1-axis showing wave propagation in [101] direction. It is necessary to write governing equations of linear piezoelasticity. Constitutive relations are as follows:

$$\sigma_{ij} = C_{ijkl}^{E}\varepsilon_{kl} - e_{ijm}E_m, \tag{1}$$

$$D_m = e_{mij}\varepsilon_{ij} + g_{mn}E_n, \tag{2}$$

in which σ_{ij} and ε_{ij} (or ε_{kl}) are the stress and strain tensors, respectively; D_m and E_m (or E_n) are components of the electric displacement and electric field ($E_m = -\partial\varphi/\partial x_m$, where φ is the electric potential); the indices i, j, k, l, m and n run from 1 to 3. According to the usual Voigt's notation, C_{ijkl}, e_{ijm} and g_{mn} can be written as 6×6, 3×6 and 3×3 matrices standing for the elasticity, piezoelectricity, and dielectricity tensors, respectively. Equilibrium equations are $\sigma_{ij,j}=0$ and $D_{i,i}=0$. It is assumed that the material is free of body forces and inertial effects as well as body electric charge.
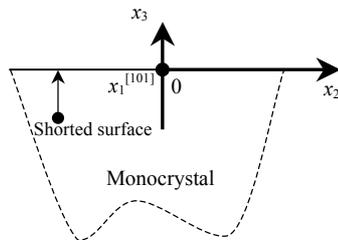
Fig.1 The coordinate system for monocrystal with the open surface or surface metallization, where the x_1-axis is directed perpendicular to the figure plane

The motion equation of an elastic medium is written as follows:

$$\rho\frac{\partial^2 U_i}{\partial t^2} = \frac{\partial\sigma_{ik}}{\partial x_k}, \tag{3}$$

where ρ and U_i denote the material density and displacement components; t is time. Using Eqs.(1)~(3) and $\varphi=U_4$, one can write the coupled equations of motion for a piezoelectric medium as follows:

$$\left.\begin{array}{l} \rho\dfrac{\partial^2 U_i}{\partial t^2} = C_{ijkl}\dfrac{\partial^2 U_l}{\partial x_j \partial x_k} + e_{kij}\dfrac{\partial^2 U_4}{\partial x_j \partial x_k}, \\[3mm] e_{ijk}\dfrac{\partial^2 U_k}{\partial x_i \partial x_j} - g_{ij}\dfrac{\partial^2 U_4}{\partial x_i \partial x_j} = 0. \end{array}\right\} \tag{4}$$

Solutions of the homogeneous partial differential Eq.(4) of the second order are found in the following plane wave view: $U_i = U_i^0 \exp[j(\mathbf{kr} - \omega t)]$, where the index i runs from 1 to 4; U_i^0 is an initial amplitude; $\mathbf{kr}$ denotes the scalar multiplication of two vectors; ω is the angular frequency. $\{k_1, k_2, k_3\}=k\{n_1, n_2, n_3\}$ are the components of the wavevector $\mathbf{k}$ and $\{x_1, x_2, x_3\}$ are the components of the real space vector $\mathbf{r}$, and $\{n_1, n_2, n_3\}$ are the so-called directional cosines.

The coupled equations of motion can be readily written in the following simplified form, leaving only equations for waves with polarization perpendicular to the sagittal plane as well as non-zero components of the material tensors:

$$\left.\begin{array}{l} \rho\dfrac{\partial^2 U_2}{\partial t^2} = C_{44}\left(\dfrac{\partial^2 U_2}{\partial x_1^2} + \dfrac{\partial^2 U_2}{\partial x_3^2}\right) + e_{16}\dfrac{\partial^2 \varphi}{\partial x_1^2} + e_{34}\dfrac{\partial^2 \varphi}{\partial x_3^2}, \\[3mm] e_{16}\dfrac{\partial^2 U_2}{\partial x_1^2} + e_{34}\dfrac{\partial^2 U_2}{\partial x_3^2} - g_{11}\left(\dfrac{\partial^2 \varphi}{\partial x_1^2} + \dfrac{\partial^2 \varphi}{\partial x_3^2}\right) = 0. \end{array}\right\} \tag{5}$$

In Eq.(5), the mechanical displacement component U_2 is directed along the x_2-axis (Fig.1):

$$U_{2,4} = U_{2,4}^0 \exp[jk(n_1 x_1 + n_3 x_3 - V_{ph}t)], \tag{6}$$

using the phase velocity definition such as $V_{ph}=\omega/k$. For piezoelectric cubic crystals, many propagation directions being perpendicular to [010] direction can

exist giving $C_{44}=C_{66}$ and $g_{11}=g_{33}$. It is also possible to cut a cubic crystal in order to study wave propagation in [101] direction with $e_{14}=e_{36}=0$ and the non-zero piezoelectric constants $\{e_{16}, e_{34}\}$ that is shown in Eq.(5).

Substituting the mechanical displacement U_2 and electrical potential $\varphi=U_4$ of Eq.(6) into Eq.(5), the equations of motion can be readily written in the well-known tensor form, using corresponding components of the modified Green-Christoffel tensor: $GL_{22}=C_{44}(1+n_3^2)$, $GL_{24}=GL_{42}=e_{16}+e_{34}n_3^2$, and $GL_{44}=-g_{11}(1+n_3^2)$ with $n_3=k_3/k$. That gives the following system of two homogeneous equations:

$$\begin{pmatrix} GL_{22}-C_{44}(V_{ph}/V_{t4})^2 & GL_{24} \\ GL_{42} & GL_{44} \end{pmatrix}\begin{pmatrix} U_2^0 \\ \varphi^0 \end{pmatrix}=0. \quad (7)$$

In Eq.(7), the directional cosines are defined as follows: $n_1\equiv1$, $n_2\equiv0$ and $n_3=n_3$. Equaling to zero the matrix determinant in Eq.(7), the suitable phase velocity V_{ph} satisfying boundary conditions discussed in the next section and four polynomial roots $n_3^{(p)}(V_{ph})$, as well as the functions $U_2^0(V_{ph})$ and $\varphi^0(V_{ph})$ can be found. For example, the functions can be taken in the following form: $\varphi^0=GL_{42}$ and $U_2^0=-GL_{44}$.

Substituting $m_3=(1+n_3^2)$ in Eq.(7) and using the piezoelectric constants $e_{16}=-e_{34}$ for [101] direction, the following polynomial can be introduced from Eq.(7):

$$(1+K_e^2)m_3^2-Bm_3+4K_e^2=0, \quad (8)$$
$$\text{with} \quad B=(V_{ph}/V_{t4})^2+4K_e^2,$$

where K_e^2 is the so-called static coefficient of the electromechanical coupling (CEMC), $K_e^2=e_{16}^2/(C_{44}g_{11})$. Note that the speed V_t of the bulk SH-wave is:

$$V_t=V_{t4}(1+K_e^2)^{1/2}. \quad (9)$$

Two roots of Eq.(8) are as follows:

$$m_3^{(1,2)}=\frac{-B\pm\sqrt{B^2-16K_e^2(1+K_e^2)}}{2(1+K_e^2)}, \quad (10)$$

giving four polynomial roots of Eq.(7) representing eigenvalues:

$$n_3^{(1,2,3,4)}=\pm\sqrt{-1+m_3^{(1,2)}}. \quad (11)$$

Note that for each eigenvalue n_3 there is the so-called eigenvector $\{U_2^0, \varphi^0\}$.

Further analyzing the roots for [101] propagation direction in Eqs.(10) and (11), it can be found that all complex roots will be calculated when the expression under square root sign in Eq.(10) is negative. That fulfills for velocities V_{ph} being less than some velocity V_a obtained solving the following equation $B^2-16K_e^2(1+K_e^2)=0$ and defined by the following formula:

$$V_a=a_KV_{t4} \quad \text{with} \quad a_K=2\sqrt{K_e\sqrt{1+K_e^2}-K_e^2}. \quad (12)$$

It is clearly seen in Eq.(12) that the factor a_K is a function of the CEMC K_e^2 together with the other function $f(K_e^2)=(1+K_e^2)^{1/2}$ from Eq.(9). The function $a_K(K_e^2=K_0^2=1/3)$ approaches the function $f(K_e^2)=(1+K_e^2)^{1/2}$ giving the following equality $V_a=V_t$, and only complex polynomial roots can exist for $V_{ph}<V_a$. The CEMC $K_0^2=1/3$ is readily found by substituting the velocity V_t from Eq.(9) to replace the phase velocity V_{ph} in equation $B^2-16K_e^2(1+K_e^2)=0$. Note that for $K_e^2<K_0^2$ there are all imaginary roots for $V_{ph}>V_a$, but a giant $K_e^2>K_0^2$ gives real roots for $V_{ph}>V_a$. It is also noted that only complex/imaginary roots with negative imaginary parts are chosen in order to have wave damping towards depth of a crystal corresponding to negative values of the x_3-axis shown in Fig.1. Probably, surface waves cannot be found in the cubic crystals with a giant $K_e^2>1/3$ in the V_{ph}-range: $V_a<V_{ph}<V_t$. Here there are two real roots for $V_{ph}>V_t$. It is thought that a great K_e^2 can be observed in complex compounds, as well as in simple materials including piezoelectric cubic crystals. For instance, the classic ferroelectric $PbTiO_3$ has been known to have a single ferroelectric tetragonal (T) to paraelectric cubic phase transition with increased temperature or pressure. Wu and Cohen (2005) studying $PbTiO_3$ discussed an unexpected tetragonal-to-monoclinic-to-rhombohedral-to-cubic phase transition sequence induced by hydrostatic pressure and a morphotropic phase boundary in a pure compound.

BOUNDARY CONDITIONS FOR SH-WAVES

Boundary conditions for studying SH-waves in monocrystals are based on several requirements which must be satisfied. There is the single mechanical boundary condition for the normal component of the stress tensor σ_{32} such as $\sigma_{32}=0$ at $x_3=0$, where

$$\sigma_{32} = \sum_{p=1,2} F^{(p)}[C_{44}k_3^{(p)}U_2^{(p)} + e_{34}k_3^{(p)}U_4^{(p)}]. \quad (13)$$

Also, there are two electrical boundary conditions: continuity of the normal component D_3 of the electrical displacements at $x_3=0$ being the interface between vacuum (D_3^{f}) and the crystal surface, where

$$\left.\begin{aligned} D_3 &= \sum_{p=1,2} F^{(p)}[e_{34}k_3^{(p)}U_2^{(p)} - g_{33}k_3^{(p)}U_4^{(p)}], \\ D_3^{\mathrm{f}} &= -F^{(0)}\phi_0^{\mathrm{f}}\mathrm{j}k_1g_0, \end{aligned}\right\} \quad (14)$$

and continuity of the electrical potential $U_4=\phi$ at $x_3=0$ ($\phi=\phi^{\mathrm{f}}$), where

$$\phi = \sum_{p=1,2} F^{(p)}\phi^{(p)} \quad \text{and} \quad \phi^{\mathrm{f}} = F^{(0)}\phi_0^{\mathrm{f}}. \quad (15)$$

Therefore, the boundary conditions determinant (BCD) for the case of free surface can be readily written from matrix view as shown in Eq.(16).

The BCD for the metallized surface can be also written from matrix view as shown in Eq.(17).

The complete mechanical displacement U_2^{Σ} and electrical potential $\varphi^{\Sigma}=U_4^{\Sigma}$ are written in the plane wave view as follows:

$$U_{2,4}^{\Sigma} = \sum_{p=1,2} F^{(p)}U_{2,4}^{0(p)} \exp[\mathrm{j}k(n_1x_1 + n_3^{(p)}x_3 - V_{\mathrm{ph}}t)]. \quad (18)$$

The weight functions $F^{(1)}$ and $F^{(2)}$ are readily found from Eq.(16), which can give the same eigenvectors

$\{U_2^{0(1)}, \varphi^{0(1)}\}$ and $\{U_2^{0(2)}, \varphi^{0(2)}\}$ for two equal eigenvalues $n_3^{(1)}=n_3^{(2)}$ and hence, $F^{(1)}=-F^{(2)}$. It is obvious that for this case the weight factors $F^{(1)}=-F^{(2)}$ will zero the complete mechanical displacement U_2^{Σ} and electrical potential φ^{Σ} in Eqs.(16) and (17) giving "latent" characteristics in Eq.(18). On the other hand, unequal eigenvalues $n_3^{(1)}$ and $n_3^{(2)}$ give different eigenvectors $\{U_2^{0(1)}, \varphi^{0(1)}\}$ and $\{U_2^{0(2)}, \varphi^{0(2)}\}$. Concerning experimental measurements of surface acoustic waves, it is also thought that some elements of crystals symmetry (screw axis or glide reflection) must be broken near the surface. The same relates to simple reflections and axis if the surface restricts the crystal in such a way that it breaks some simple elements of the crystals class group. Thus, to experimentally distinguish different types of surface waves is difficult and not unequivocal.

RESULTS AND DISCUSSIONS

Calculations of the phase velocity V_{ph}, the velocities V_a, V_{t4} and V_t, as well as the CEMC K_{e}^2 were carried out for different piezoelectric cubic crystals: Chalcogenides Tl_3VS_4 and Tl_3TaSe_4 (cubic, class $\bar{4}3m$), and Bismuth Titanate $Bi_{12}TiO_{20}$ (cubic, class 23). For the ternary thallium Chalcogenide Tl_3TaSe_4, material constants for [100] direction are as follows: ρ=7280 [kg/m^3], C_{44}=0.41×10^{10} [N/m^2], e_{14}=0.32 [C/m^2], and $|g_{11}|/|g_0|$=10.1. g_0 is the dielectric constant of vacuum, g_0=0.08854×10^{-10} [F/m]. Note that difference between [101] and [100] directions are confined in the piezoelectric constants: $|e_{16}|^{[101]}=|e_{14}|^{[100]}$. The same material constants for Tl_3VS_4 are: ρ=6140 [kg/m^3], C_{44}=0.47×10^{10} [N/m^2], e_{14}=0.55 [C/m^2], and $|g_{11}|/|g_0|$=34.8. These material constants give great CEMCs $K_{\mathrm{e}}^2(Tl_3TaSe_4)=(e_{16})^2/(C_{44}g_{11})$ ~0.2793 and $K_{\mathrm{e}}^2(Tl_3VS_4)$~0.2089. All the wave characteristics were calculated with an accuracy of about 1 μm/s that is useful and allows distinguishing V_{ph}-solutions when they are close to each other. The

$$\begin{pmatrix} C_{44}k_3^{(1)}U_2^{(1)} + e_{34}k_3^{(1)}U_4^{(1)} & C_{44}k_3^{(2)}U_2^{(2)} + e_{34}k_3^{(2)}U_4^{(2)} \\ e_{34}k_3^{(1)}U_2^{(1)} - (g_{33}k_3^{(1)} - \mathrm{j}g_0k_1)U_4^{(1)} & e_{34}k_3^{(2)}U_2^{(2)} - (g_{33}k_3^{(2)} - \mathrm{j}g_0k_1)U_4^{(2)} \end{pmatrix}\begin{pmatrix} F^{(1)} \\ F^{(2)} \end{pmatrix} = 0. \quad (16)$$

$$\mathrm{j}g_0k_1\begin{pmatrix} C_{44}k_3^{(1)}U_2^{(1)} + e_{34}k_3^{(1)}U_4^{(1)} & C_{44}k_3^{(2)}U_2^{(2)} + e_{34}k_3^{(2)}U_4^{(2)} \\ U_4^{(1)} & U_4^{(2)} \end{pmatrix}\begin{pmatrix} F^{(1)} \\ F^{(2)} \end{pmatrix} = 0. \quad (17)$$

wave characteristics for Tl_3TaSe_4 are as follows: $V_{t4} \sim 750.4577358$ m/s, $V_t \sim 848.8104580$ m/s, and $V_a \sim 846.9869546$ m/s. The speed V_t of the bulk SH-wave is slower than 1000 m/s and the value of V_a is close to V_t because K_e^2 is close to $K_0^2 = 1/3$. According to the recent publication (Gulyaev and Hickernell, 2005), SH-SAWs (for instance, the surface BG-waves) cannot exist in piezoelectric cubic crystals. Hence, any found V_{ph}-solutions below the speed V_t for the boundary conditions' determinants (BCDs) in Eqs.(16) and (17), except in the case of V_a with two equal roots, will represent new-wave solutions of SAWs. The V_{ph}-solutions are found when values of the BCDs fall to zero. Indeed, new SAWs can be found in cubic crystals with strong piezoelectric effect for electrical boundary conditions of both free and metallized surfaces. For the strongest piezoelectrics Tl_3TaSe_4 of the treated cubic crystals, the existence possibility of new SAWs for both electrical boundary conditions is obvious that allows evaluation of the coefficient of electromechanical coupling:

$$K^2 = 2(V_{new} - V_{new,m})/V_{new}, \qquad (19)$$

where V_{new} and $V_{new,m}$ are the velocities of new SAWs for the free and metallized surfaces, respectively. The velocities $V_{new} \sim 848.125556$ m/s and $V_{new,m} \sim 828.335498$ m/s for the crystal Tl_3TaSe_4 give $K^2 \sim 0.04667$, and the behavior of corresponding BCDs is shown in Fig.2. Note that here the new-SAW velocity V_{new} can be approximated with $V_{new}=(V_t+V_a)/2$, because the value of V_{new} is situated between the values of V_t and V_a.
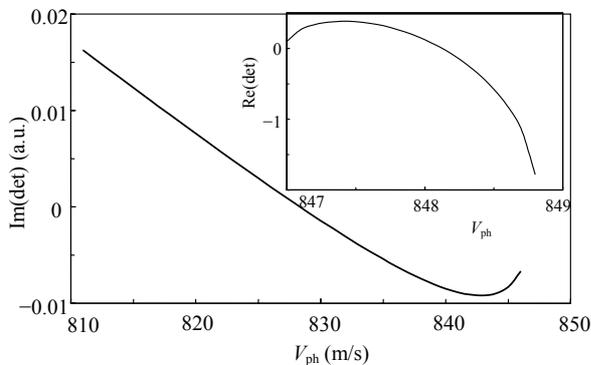
The V_{ph}-solutions for both the BCDs are shown in Fig.3 for the other strong piezoelectrics Tl_3VS_4 with the value of K_e^2 being significantly less than the one for Tl_3TaSe_4. The characteristics of Tl_3VS_4 are: $V_{t4} \sim 874.9127458$ m/s, $V_t \sim 961.9607843$ m/s, and $V_a \sim 948.1841318$ m/s. The calculated velocities of the new SAWs are $V_{new} \sim 961.927246$ m/s and $V_{new,m} \sim 947.491302$ m/s giving about 1.5 times decrease in the CEMC, $K^2(Tl_3VS_4) \sim 0.030$, calculated with Eq.(19). Here the velocity $V_{new,m}$ is still significantly less than V_t and is about V_a. On the other hand, it is clearly seen from the above written values of V_{new} and V_t that they are close to each other for the large value of $K_e^2(Tl_3VS_4) \sim 0.2089$, which is about two times greater than that for the cubic crystal $Bi_{12}TiO_{20}$: $K_e^2(Bi_{12}TiO_{20}) \sim 0.1118$. That is true for the other crystals of class 23, $Bi_{12}SiO_{20}$ and $Bi_{12}GeO_{20}$, which possess smaller values of $K_e^2(class\ 23) \sim 0.10$ to 0.15 (Zakharenko, 2005). Fig.4 shows the BCD behavior for the cubic crystal $Bi_{12}TiO_{20}$, using the following material constants taken from (Kamenov *et al.*, 2000): $\rho=11200$ [kg/m^3], $C_{44}=2.60 \times 10^{10}$ [N/m^2], $e_{14}=1.10$ [C/m^2], and $g_{11}=4.16138 \times 10^{-10}$ [F/m]. The $Bi_{12}TiO_{20}$ material constants result in relatively high velocities $V_{t4} \sim 1523.62350$ m/s, $V_t \sim 1606.562692$ m/s, and $V_a \sim 1495.282953$ m/s being about two times greater than those for the Chalcogenides. The velocity $V_{new} \sim 1606.556882$ m/s here is very close to the speed V_t, but can still be distinguished in the calculations using the set accuracy of about 1 μm/s. The velocity $V_{new,m} \sim 1598.414906$ m/s is significantly less than V_t, but greater than V_a, which means that $V_{new,m}$ can also reach V_t. Using the calculated velocities V_{new} and

Fig.2   The dependence of the boundary conditions determinants (BCD) on the phase velocity V_{ph} for [101]-direction of wave propagation in the cubic crystal Tl_3TaSe_4 with the metallized surface. The insertion shows the solution of Re(det)×10^{-3} for the open surface
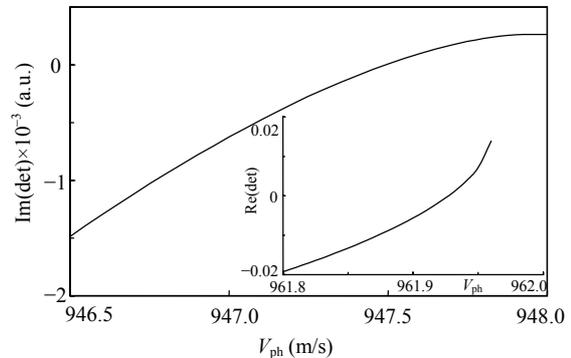
Fig.3   The dependence of the boundary conditions determinants (BCD) on the phase velocity V_{ph} for [101]-direction of wave propagation in the cubic crystal Tl_3VS_4 with the metallized surface. The insertion shows the solution of Re(det) for the open surface
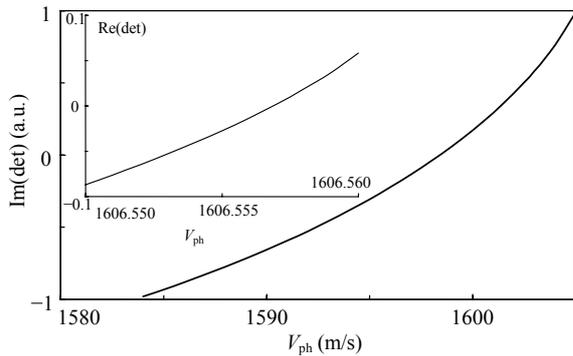
Fig.4 The dependence of the boundary conditions determinants (BCD) on the phase velocity V_{ph} for [101]-direction of wave propagation in $Bi_{12}TiO_{20}$ with the metallized surface. The insertion shows the Re(det) solution for the open surface

$V_{new,m}$, the evaluated value of the K^2 from Eq.(19) is as high as $K^2(Bi_{12}TiO_{20})\sim0.010$ that is only 1%. It is thought that the bulk SH-wave with the speed V_t is unstable and can be readily treated as the SH-SAWs for the weaker piezoelectrics such as the crystals of class 23. Indeed, the penetration depth here can reach macroscopic distances towards the crystal depth.

CONCLUSION

In this report of theoretical work, the phase velocity V_{ph} and coefficient of electromechanical coupling K^2 were calculated for new SH-SAWs propagating in [101] direction on the surface of piezoelectric cubic crystals, in which the surface Bleustein-Gulyaev waves cannot propagate. For the Chalcogenide Tl_3TaSe_4 with the greatest CEMC $K_e^2\sim1/3$, the velocity V_{new} for the new SH-SAWs is significantly less than the speed V_t of the bulk SH-waves, $V_D=V_{new}-V_t\sim0.7$ m/s for the free surface, while the difference V_D for the crystal Tl_3VS_4 with the CEMC $K_e^2\sim1/5$ is $V_D\sim0.03$ m/s. For the Bismuth Titanate possessing the smallest value of the CEMC $K_e^2(Bi_{12}TiO_{20})\sim1/10$ concerning the studied crystals, the difference V_D is very small and equals to ~0.007 m/s which already makes difficulties for numerically finding the phase velocity V_{new} of new SH-SAWs, as

well as for distinguishing it from the bulk SH-wave propagating with the speed V_t. Using the surface metallization, the corresponding differences V_D for the studied crystals are as follows: $V_D(Tl_3TaSe_4)\sim20.5$ m/s ($V_{new,m}\ll V_a$), $V_D(Tl_3VS_4)\sim14.5$ m/s with $V_{new,m}\sim V_a$ and $V_D(Bi_{12}TiO_{20})\sim8$ m/s ($V_{new,m}\gg V_a$). Also, the additional solutions for the V_a, which is significantly less than the speed V_t for weakly-piezoelectric cubic crystals, give latent displacements or zero ones. However, it is thought that different surface perturbations can result in visualization of the displacements that must be experimentally verified for sensor application.

References

Bleustein, J.L., 1968. A new surface wave in piezoelectric materials. *Applied Physics Letters*, **13**(12):412-413. [doi:10.1063/1.1652495]

Gulyaev, Y.V., 1969. Electroacoustic surface waves in solids. *Soviet Physics Journal of Experimental and Theoretical Physics Letters*, **9**:37-38 (in Russian).

Gulyaev, Y.V., Hickernell, F.S., 2005. Acoustoelectronics: history, present state and new ideas for a new era. *Acoustical Physics Reports*, **51**(1):101-110 (in Russian).

Henaff, J., Feldmann, M., Kirov, M.A., 1982. Piezoelectric crystals for surface acoustic waves (Quartz, LiNbO$_3$, LiTaO$_3$, Tl$_3$VS$_4$, Tl$_3$TaSe$_4$, AlPO$_4$, GaAs). *Ferroelectrics*, **42**:161-185.

Kamenov, V.P., Hu, Y., Shamonina, E., Ringhofer, K.H., Gayvoronsky, V.Y., 2000. Two-wave mixing in (111)-cut Bi$_{12}$SiO$_{20}$ and Bi$_{12}$TiO$_{20}$ crystals: characterization and comparison with the general orientation. *Phys. Review E*, **62**(2):2863-2870. [doi:10.1103/PhysRevE.62.2863]

Kessenikh, G.G., Shuvalov, L.A., 1982. Transverse surface waves in piezoelectric crystals of classes 622 and 422. *Ferroelectrics*, **42**:149-152.

Maerfeld, C., Tournois, P., 1971. Pure shear elastic surface wave guide by the interface of two semi-infinite media. *Applied Physics Letters*, **19**(4):117-118. [doi:10.1063/1.1653836]

Wu, Z., Cohen, R.E., 2005. Pressure-induced anomalous phase transitions and colossal enhancement of piezoelectricity in PbTiO$_3$. *Physical Review Letters*, **95**:037601. [doi:10.1103/PhysRevLett.95.037601]

Zakharenko, A.A., 2005. Love type waves in layered systems consisting of two piezoelectric cubic crystals. *Journal of Sound and Vibration*, **285**(4-5):877-886. [doi:10.1016/j.jsv.2004.08.044]